SPE-173238-MS

Spatial-Temporal Tensor Decompositions for Characterizing Control-Relevant Flow Profiles in Reservoir Models

E. Insuasty, Eindhoven University of Technology (EUT); P.M.J. Van den Hof, S. Weiland, EUT; J.D. Jansen, Delft University of Technology

This paper was prepared for presentation at the SPE Reservoir Simulation Symposium held in Houston, Texas, USA, 23–25 February 2015.

Abstract

This paper considers the use of spatial-temporal (tensor) decompositions for the compact representations of saturation patterns in reservoir models. Reservoir flow patterns, in the sense of evolution of saturation patterns over time, can be considered to drive the economic performance of reservoirs as they drive the ultimate recovery. This makes the reservoir flow pattern a natural dissimilarity measure between models in the context of production optimization. We show that the application of multilinear algebra techniques allows the construction of low-complexity representations of the essential saturation patterns. The reservoir flow patterns are stored in large-scale multidimensional arrays, and tensor decompositions can be effectively used to describe the spatial-temporal behavior of the reservoir flow patterns. The dimensionality of the reservoir flow patterns can be substantially reduced, showing that a small number of spatial-temporal basis functions are required to characterize the dominant features. When applying the tensor decompositions to flow profiles of an ensemble of realizations they can be used for clustering models with similar dynamical properties, by allowing a fast calculation of a flow-relevant dissimilarity measure between realizations. For large ensembles of realizations they can lead to considerable computational advantages in (robust) optimization. This is illustrated by using a gradient-based technique to maximize Net Present Value (NPV) in water flooding for an ensemble of realizations. Besides in reducing ensemble sizes the resulting tools have potential use in constructing reduced order models.

Introduction

The increasing demand for energy has encouraged the use of improved production strategies for conventional oil and gas resources. In this context, several studies have indicated a significant scope for reservoir model-based life-cycle optimization of ultimate recovery or NPV, especially when combined with computer-assisted history matching leading to a closed-loop reservoir management (CLRM) approach; see e.g. Jansen et al. (2008), Sarma et al. (2008) or Chen et al. (2009). To properly include the effect of uncertainty it is important to perform both the history matching and the life-cycle optimization using ensembles of multiple realizations. The combination of iterative optimization and history matching procedures with the need to use multiple realizations makes CLRM into a computationally very demanding process for realistically-sized reservoir models. Several authors have therefore studied the

reduction of the dynamical (number of states) and structural (parameterizations of geological structures) complexities of reservoir models, and their implication for control and parameter estimation. Van Doren et al. (2013) have analyzed the system theoretical properties of a two-phase reservoir model, where controllable and observable states belong to a small subset of the original state space. The reduced set of controllable states is related to the sets of possible state trajectories that can be obtained with a particular production strategy. This indicates that full-scale reservoir models are generally more complex than necessary for the purpose of production optimization. Vakili-Ghahani and Jansen (2012) have exploited system theoretical concepts to define the level of refinement of spatial grids in reservoir models, where spatial location with the most controllable and observable states are meshed finer than other regions of the spatial domain. On the other hand, Tavakoli et al. (2010) and Van Doren et al. (2011) have used parameterizations of geological structures with sensitivity analyses that indicate that only a reduced set of parameters can be validated from data. From the systems and control perspective, these studies are evidence that grid-based reservoir models describe the flow dynamics at a level of detail that is too high for the computation of model-based production strategies and for data-based parameter validation. Hence, there is a need for reduced-complexity reservoir models that retain maximal information on the dynamical aspects that are most relevant for model-based optimization.

When using reservoir realizations as a basis for model-based optimization of NPV in water flooding, one would like to discriminate between realizations that have essentially different dynamical behavior in NPV performance. In other words, there is a need for a control-relevant dissimilarity measure between geological realizations for model-based operation of oil reservoirs. For this purpose, it seems relevant to develop a measure that relates the dynamical properties of the reservoir to its financial performance.

Traditionally, the key elements of model-based reservoir management are a set of reservoir parameters, a financial measure of performance and a production strategy. This is, a large number of geological realizations (*an ensemble*) to quantify the lack of knowledge on the subsurface properties, the NPV and the operational injection/production well settings, which intends to maximize a performance measure. In this context, several authors have used dissimilarity measures based on these elements to quantify the static and dynamical variability of the ensemble. Caers et al. (2010) have used the difference in permeability fields as a measure of dissimilarity between geological realizations. This has been performed by defining a metric space to compare and cluster geological models that share common geological features. However, it is well known that reservoir models with highly dissimilar permeability and porosity fields might generate similar flow rates at production wells, *i.e.*, different geological realizations of oil reservoirs may have similar I-O behavior and may reproduce nearly identical production data. From an operational perspective, a distance between reservoir models based permeability fields is not able to capture the dynamical variability of the ensemble, as models with different permeability fields may lead to similar reservoir flow patterns.

For production optimization, the use of the final NPV as a control-relevant dissimilarity measure between realizations might be considered as natural. However, it is well known that the final NPV is not able to capture the relevant aspects of the reservoir flow patterns associated with a particular production strategy. Van Essen et al. (2009) have shown that although reservoir realizations might look different from a geological perspective, they may generate the same NPV with the implementation of their own optimal production strategies. Jansen et al. (2009) have made a similar observation, by pointing out the levels of redundancy in the input space, where different control inputs and geological configuration of parameters may lead to nearly identical NPV performance in a closed-loop setting.

From the previous analysis, it follows that control-relevant dissimilarity measures between models based on geological parameters (*permeability and porosity fields*) and NPV have their limitations. On one hand, the final NPV after the production stage is a static measure, which does not reflect the temporal build-up of the cash flow during production. The build-up trajectory of NPV is an important quantity to be considered, especially when short-term revenues are required because of geological and economical

uncertainty, fluctuations of oil price and discount rates. On the other hand, large dissimilarities of geological parameters may not necessarily imply substantial effects on the outcome of reservoir simulators and on the computation of optimal production strategies. To exemplify this, upscaling of high resolution geological models, as is presented in Durlofsky (2005), is evidence that reservoir flow dynamics lie in low dimensional spaces, and that dissimilar reservoir models may have similar dynamical performance in terms of flow dynamics. For the reasons exemplified before, we observe that temporal evolution of NPV and the full solution (*saturation patterns*) of the reservoir simulators are crucial, first to determine performance evaluation of reservoir management strategies for different realizations, and second, to device field development plans such as well design and construction, economics and risk assessment.

Temporal evolution of the oil recovery from a reservoir and therefore of the resulting cash flow depends on the selected production strategy. In addition, this strategy directly influences the fluid behavior, that is, reservoir flow patterns, which we define as the temporal evolution of the oil, water and gas saturations in the reservoir. Reservoir flow patterns are a function of the driving forces in the reservoir, i.e. viscous, capillary and gravity forces. In this paper we restrict our attention to water flooding situations in which case the reservoir flow patterns are directly linked to the injection and production rates in the wells. The ultimate recovery of a reservoir is therefore strongly related to the reservoir flow patterns. This makes the saturation patterns a natural dissimilarity measure between reservoir models in the context of model-based operation and optimization of oil reservoirs. Alpak et al. (2010) have proposed a rapid characterization of the geological uncertainty based on the fast computation of the streamline pattern for the ensemble, and use it as a dissimilarity measure to cluster geological realizations that have similar dynamical performance in terms of the streamlines solution.

In this work we consider the use of full reservoir flow patterns as the dissimilarity measure between geological realizations in an optimal production strategy setting, in order to capture the most relevant process dynamics for control.

Reservoir flow patterns are numerical solutions of the pressure and transport partial differential equations (PDEs) (Aziz and Settari (1979)), and represent the temporal evolution of dependent variables (*saturations and pressure*) in the spatial domain of the reservoir. Numerical methods for PDEs discretize the spatial domain (typically $10^5 \sim 10^6$ grid blocks), whereafter time stepping algorithms generate discrete time series (known as trajectories) for pressure and saturation. In this work, we propose a novel low-order characterization of reservoir flow patterns.

Various methods exist for characterizing such reservoir flow patterns. Classical methods use matrix decompositions, such as the Singular Value Decomposition (SVD), to extract the most relevant features of numerical solutions of PDEs. This approach has some limitations. In particular, they lose the spatial-temporal structure of numerical solutions which may have serious implications when characterizing flow profiles in low-dimensional spaces. When classical SVD is applied to a snapshot matrix, sets of orthonormal basis vectors are found that average the energy of solutions in time. See, e.g., Heijn et al. (2004), Markovinovic and Jansen (2006), Cardoso et al. (2009), Krogstad (2011) and Kaleta et al. (2011) for applications of such SVD-based flow characterization and POD model order reduction techniques. This energy averaging causes a loss of information for some of the relevant features of the solutions. In order to improve the quality of the characterization of reservoir flow patterns, novel tensor techniques have been recently investigated for the decomposition of numerical solutions of PDEs. Some of these techniques keep the spatial structure intact, see e.g., Shekhawat and Weiland (2014).

The principal features of reservoir flow patterns in reservoir engineering are: large-scale structures, multivariable signals, different time scales, variable units and a spatial-temporal nature. The last feature of reservoir flow patterns allows an efficient storage of the flow-relevant data structures in tensors, *i.e.*, in multidimensional arrays. This creates a clear separation in time, space and variables. Particularly, when using an ensemble of reservoir models to quantify the geological uncertainty, an extra dimension (model

dimension) in the tensor representation can be included to efficiently store the numerical solutions of multiple models.

Tensor decompositions and tensor analysis constitute a largely unexplored subject in reservoir engineering. For the characterization of geological parameters, Afra and Gildin (2013); Afra et al. (2014) have performed low rank approximations of permeability fields using a tensor decomposition, and Gildin and Afra (2014) who have used low rank tensor representations of permeability fields for efficient data assimilation. For the reduction of dynamical complexity of reservoir models, Insuasty et al. (2015) have introduced a novel framework for reduced order modeling in reservoir engineering, where tensor decompositions and representations of flow profiles are used to characterize empirical projection spaces for the reduced order model. In this work, we apply state of the art tensor decomposition techniques to characterize flow profiles in low dimensional spaces with an application to production optimization under uncertainty. This paper is organized as follows: In the section Theory, we review the classical and tensor methods for flow characterization, flow-based dissimilarity measures, visualization techniques and robust optimization. In the section Methodology, we describe the steps for tensor-based flow characterization. In the section Results, we illustrate the application of the methodology for flow characterization of single and multiple reservoir models and in section Discussion, we make observations on the results, particularly on the selection of adequate production strategies for flow characterization.

Theory

In this section, we provide the tensor-based techniques that are presently used to find compact representations of high-dimensional data structures. We discuss visualization techniques for high dimensional data and give an overview of a technique for production optimization under uncertainty.

Classical Singular Value Decomposition of a Snapshot Matrix

Consider a two-dimensional (2D) rectangular reservoir model with $I \cdot J$ (i.e. I times J) grid blocks, simulated for K time steps with a discrete time stepping algorithm. The dynamic variables in each grid block are represented generically as $(I \cdot J)$ x 1 vectors x with elements that could represent either pressures or saturations. A number of K snapshot vectors x_k is collected at time steps $k = 1, 2, \ldots, K$ where K may be less or equal to the total number of simulation time steps. The $(I \cdot J)$ x K matrix

$$\mathbf{X} = \begin{bmatrix} \mathbf{x}_1 & \mathbf{x}_2 & \cdots & \mathbf{x}_K \end{bmatrix}, \tag{1}$$

can now be decomposed using an SVD as (Eckart and Young (1936))

$$\mathbf{X} = \Phi\Sigma\Psi^{\top} = \sum_{r=1}^{R} \varphi_r \sigma_r \psi_r^{\top} = \sum_{r=1}^{R} \sigma_r \underbrace{\varphi_r \otimes \psi_r}_{\Theta_r}, \tag{2}$$

where Φ and ψ are $(I \cdot J) \times (I \cdot J)$ and $K \times K$ orthogonal matrices containing the left and right singular (column) vectors ϕ and ψ, Σ is an $(I \cdot J) \times K$ rectangular diagonal matrix of singular values σ, and R is the rank of X where $R \leq K < I \cdot J$ in typical reservoir simulation applications. The last eqauality in Eq. 2 indicates that X can be decomposed as the sum of R rank-one matrices $\Theta_r = \varphi_r \psi_r^{\mathrm{T}} = \varphi_r \otimes \psi_r$ where the symbol $\otimes$ denotes the tensor or outer product over a vector space. A low-rank approximation $\hat{\mathbf{X}}$ of X can be obtained by writing Eq. 2 as

$$\mathbf{X} = \hat{\mathbf{X}} + \mathbf{X}_{\varepsilon} = \underbrace{\sum_{r=1}^{\hat{R}} \sigma_r \varphi_r \otimes \psi_r}_{\hat{\mathbf{X}}} + \underbrace{\sum_{r=\hat{R}+1}^{R} \sigma_r \varphi_r \otimes \psi_r}_{\mathbf{X}_{\varepsilon}}, \tag{3}$$

where $\hat{R} < R$ and where X_{ε} is the error term.

Tensor Decomposition of a Snapshot Tensor

Alternatively we can collect $I \times J$ snapshot matrices X_k (instead of $(I \cdot J) \times 1$ snapshot vectors), and stack them in a three-dimensional tensor S of size $I \times J \times K$. It can be shown that, in analogy to matrix decomposition in Eq. 2, the tensor S can be decomposed as (Kolda and Bader (2009))

$$\mathbf{S} = \sum_{i=1}^{I}\sum_{j=1}^{J}\sum_{k=1}^{K} \sigma_{ijk} \underbrace{\varphi_i \otimes \psi_j \otimes \chi_k}_{\Theta_{ijk}}, \tag{4}$$

where $\Theta_{ijk} = \phi_i \otimes \psi_j \otimes \chi_{\ k}$ are now rank-one tensors, and ϕ_i, ψ_j, and $\chi_{\ k}$ are orthonormal basis functions (vectors) such that, e.g., $\varphi_{i'}^{\top}\varphi_{i''} = \delta_{i'i''}$, $\psi_{j'}^{\top}\psi_{j''} = \delta_{j'j''}$ and $\chi_{k'}^{\top}\chi_{k''} = \delta_{k'k''}$ where $\delta_{w'w''}$ where $\delta_{\mathrm{w'w''}}$ is the Dirac delta function defined as

$$\delta_{w'w''} = \begin{cases} 1 & \text{if } w' = w'' \\ 0 & \text{if } w' \neq w'' \end{cases}. \tag{5}$$

The scalars σ_{ijk} are the elements of an $I \times J \times K$ core tensor, i.e. the 3D analogy of a diagonal matrix.

Approximation Error

Similar as in the matrix case, a low-rank approximation $\hat{\mathbf{S}}$ of S can be obtained by writing Eq. 4 as

$$\mathbf{S} = \hat{\mathbf{S}} + \mathbf{S}_\varepsilon = \underbrace{\sum_{i=1}^{\hat{I}}\sum_{j=1}^{\hat{J}}\sum_{k=1}^{\hat{K}} \sigma_{ijk}\varphi_i \otimes \psi_j \otimes \chi_k}_{\hat{\mathbf{S}}} + \underbrace{\sum_{i=\hat{I}+1}^{I}\sum_{j=\hat{J}+1}^{J}\sum_{k=\hat{K}+1}^{K} \sigma_{ijk}\varphi_i \otimes \psi_j \otimes \chi_k}_{\mathbf{S}_\varepsilon}, \tag{6}$$

where $\hat{I} < I, \hat{J} < J, \hat{K} < K$ and where S_ε is the error term. For instance, if a reduced set of basis functions is used to build tensor S, it can be approximated by

$$\mathbf{S} \approx \hat{\mathbf{S}} = \sum_{i=1}^{\hat{I}}\sum_{j=1}^{\hat{J}}\sum_{k=1}^{\hat{K}} \sigma_{ijk}\varphi_i \otimes \psi_j \otimes \chi_k. \tag{7}$$

Now, we can define the notion of approximation error as

$$\| \mathbf{S} - \hat{\mathbf{S}} \|_{\mathcal{F}} \quad = \quad \| \mathbf{S} \|_{\mathcal{F}} - \sum_{i=1}^{\hat{I}}\sum_{j=1}^{\hat{J}}\sum_{k=1}^{\hat{K}} \sigma_{ijk}^2 \quad = \quad \sum_{i=\hat{I}+1}^{I}\sum_{j=\hat{J}+1}^{J}\sum_{k=\hat{K}+1}^{K} \sigma_{ijk}^2. \tag{8}$$

The Frobenius norm of tensors in Eq. 8 is used to compute a relative approximation error related to the tensor approximation as follows:

$$e_{rel} = \frac{||\mathbf{S} - \hat{\mathbf{S}}||_{\mathcal{F}}}{||\mathbf{S}||_{\mathcal{F}}} = \frac{\sqrt{\sum_{i=1}^{I}\sum_{j=1}^{J}\sum_{k=1}^{K} S_{\varepsilon,ijk}^2}}{\sqrt{\sum_{i=1}^{I}\sum_{j=1}^{J}\sum_{k=1}^{K} S_{ijk}^2}} = \frac{\sqrt{\sum_{i=\hat{I}+1}^{I}\sum_{j=\hat{J}+1}^{J}\sum_{k=\hat{K}+1}^{K} \sigma_{ijk}^2}}{\sqrt{\sum_{i=1}^{I}\sum_{j=1}^{J}\sum_{k=1}^{K} \sigma_{ijk}^2}}, \tag{9}$$

where S_{ijk} and $\mathrm{S}_{\varepsilon,ijk}$ are the *ijk*-th elements of the tensors S and S_ε.

Empirical Tensor Basis and Algorithms

The description of S in (4) requires the construction of ordered orthonormal sets of basis functions for the tensor decomposition. This problem can be formulated as an optimization problem as follows

$$\begin{aligned} &\min_{\varphi_{1:I},\psi_{1:J},\chi_{1:K}} \left\| \mathbf{S} - \sum_{i=1}^{I}\sum_{j=1}^{J}\sum_{k=1}^{K} \sigma_{ijk}\varphi_i \otimes \psi_j \otimes \chi_k \right\|_{\mathcal{F}} \\ &\text{s.t.} \quad \varphi_{i'}^{\top}\varphi_{i''} = \delta_{i'i''}, \quad \psi_{j'}^{\top}\psi_{j''} = \delta_{j'j''} \quad \chi_{k'}^{\top}\chi_{k''} = \delta_{k'k''}, \end{aligned} \tag{10}$$

In literature, several algorithms have been reported to compute tensor decompositions and sets of tensor orthonormal basis functions. In this paper, we consider the *Tucker modal-rank* type of decomposition (Kolda and Bader (2009)), which defines orthonormality for the sets of vectors $\phi_{1:I}$, $\psi_{1:J}$, $\chi_{1:K}$. The *High Order SVD* (HOSVD) proposed by De Lathauwer et al. (2000a) was the first extension of a classical SVD to the multilinear case and the methodology is based on the unfolding procedure of tensors, losing

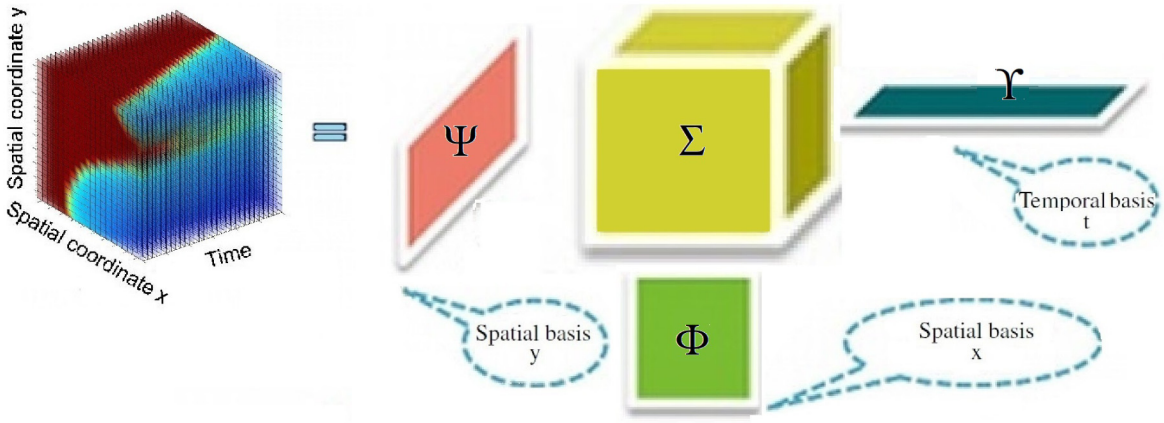

Figure 1—Schematic description for the truncation of a Tucker decomposition of a 3D tensor.

the tensor structure and performing computations in the matrix plane. The *High Order Orthogonal Iteration* (HOOI) by De Lathauwer et al. (2000b), the *Tensor SVD* proposed by Weiland and Van Belzen (2010), *Maximum Singular Value Modal Rank* (MSVM) and the *Single Directional Modal-rank decomposition* (SDM) by Shekhawat and Weiland (2014) compute singular values and vectors of tensors in a sequential way, where the singular values and vectors depend on a search direction at every decomposition level. Tensor SVD, MSVM and SDM keep the tensor structure intact in the decomposition procedure. A graphical description of the tensor decompositions considered in this paper can be seen in Fig.1.

Flow-based Dissimilarity Measure between Models

In the previous section, the use of saturation patterns as a dissimilarity measure between models has been motivated, as a way to quantify the dynamical/control variance of an ensemble of reservoir models. In addition, we exploit the spatial-temporal nature saturation patterns to find their corresponding tensor representation. In this subsection, we introduce a flow-based dissimilarity measure between two different reservoir models in the multilinear framework.

Let us assume that we have two different (reduced) snapshot tensors $\hat{\mathbf{S}}_i$ and $\hat{\mathbf{S}}_j$ corresponding to the simulated flooding response of two geological realizations of a reservoir. A measure for distance in the low dimensional space can be constructed for every pair of realizations *i, j* using Eq. 7. Let us define the tensor $\mathbf{D}_{i,j} = \hat{\mathbf{S}}_i - \hat{\mathbf{S}}_j$ then:

$$d_{ij} = ||\mathbf{D}_{i,j}||_{\mathcal{F}} = \sqrt{\sum_{a=1}^{I}\sum_{b=1}^{J}\sum_{c=1}^{K} D_{ij,abc}^2}, \tag{11}$$

where $D_{ij,abc}^2$ is the *abc*-th element of the tensor $\mathbf{D}_{i,j}$. For an ensemble of reservoir models and saturation patterns, is it possible to build a distance matrix Δ, where d_{ij} is the *ij*-th element of Δ. Then, a map showing the distance between models can be constructing using Multi-Dimensional Scaling (MDS), as it is described in the following section.

Multi-Dimensional Scaling

When having representative information for a large number of variables it is often useful to extract the dominant patterns from the data. This can be conveniently done using MDS which was introduced by Suzuki et al. (2008) and Caers et al. (2010) in the reservoir modeling community. For a description of the underlying theory, see Borg and Groenen (2005). The technique allows us to visualize the dissimilarities between a set of objects. It is based on the notion of *distances* between the *n* objects under consideration, which, in our application, are given by a distance matrix Δ as defined in the previous subsection. MDS subsequently uses an SVD-based technique to determine a low-order set of dimensionless directions in which the relative distances between the objects can be efficiently represented. In particular when

considering just two or three of the most relevant 'directions' it is possible to represent the distances between the objects graphically.

Robust Optimization

Decision making processes in the presence of model uncertainty constitute a major challenge in reservoir engineering and closed-loop reservoir management. In order to design a production strategy to account for parametric uncertainties in reservoir models, *Robust Optimization* (RO) has been applied, see Van Essen et al. (2009), Chen et al. (2012), Yasari et al. (2013) and Fonseca et al. (2015). The NPV is defined as the net cash flow along the operational life cycle of the reservoir:

$$J=\sum_{k=1}^{K}\left[\frac{\sum_{i=1}^{N_{inj}} r_{wi}\cdot(u_{wi,i})_k+\sum_{j=1}^{N_{prod}}\left[r_{wp}(y_{wp,i})_k+r_o(y_{o,j})_k\right]}{(1+b)^{\frac{t_k}{\tau}}}\cdot\Delta t_k\right] \tag{12}$$

where $u_{wi,i}$ are the injection rates (control inputs), K is the optimization horizon, Δt_k is the time step, b is the discount factor, N_{inj} and N_{prod} are the number of injectors and producers, r_{wi} and r_{wp} denote the cost of water injection and production, r_o represents the price of oil produced and $y_{wp,i}$ and $y_{o,j}$ denote the water and oil production rates (measured outputs). In RO, we maximize the average value of NPV over an ensemble of N_R realizations.

$$J_{rob}=\frac{1}{N_R}\sum_{i=1}^{N_R}J(\mathbf{u}_{1:K},\mathbf{y}^i_{1:K},\theta_i), \tag{13}$$

with gradient

$$\frac{dJ_{rob}}{d\mathbf{u}_k}=\frac{1}{N_R}\sum_{i=1}^{N_R}\frac{dJ(\mathbf{u}_{1:K},\mathbf{y}^i_{1:K},\theta_i)}{d\mathbf{u}_k},\quad k=1,2,\cdots,K, \tag{14}$$

where u_k and y_k are the input and output vectors at time step k. RO requires the computation of the numerical gradients of the cost function for every member of the ensemble and the technique can become computationally prohibitive for big ensembles of large-scale models due to the burden associated with the computational load required to compute numerical gradients and simulations. Approximation of the gradients can be done using ensemble optimization, Chen et al. (2009) and Fonseca et al. (2015), without the need of an adjoint formulation, however, the methods are even more computational expensive for large ensembles of reservoir models.

An approach for reducing the computational effort of RO is the use of reduced size flow-relevant ensembles. Yeh et al. (2014) have used fast indicators (*dynamical fingerprints*) of the dynamical behavior of reservoir models, in order to quantify the dynamical variance of an ensemble. This has been used to identify clusters of models with similar dynamical behavior, and for the generation of flow-relevant ensemble of realizations for model maturation and probabilistic history matching. In our work, flow-based dissimilarity measures are used for the generation of a reduced size flow-relevant ensembles, which is used for the efficient implementation of RO.

Methodology

In this section, we propose a methodology to characterize and compare the dynamical variability of reservoir flow patterns in a low-dimensional space. The spatial-temporal nature of the reservoir flow patterns allows a tensor representation of the oil saturation, which is exploited by the methodology in two different aspects: On one side, tensor representations allow the implementation of tensor decompositions which keep spatial correlations, that are otherwise lost when using SVD-type characterizations. On the other side, reduced-order tensor representations allow the efficient computation of flow-relevant dissimilarity measures to estimate the similarity of two different geological realizations with respect to their dynamical variability.

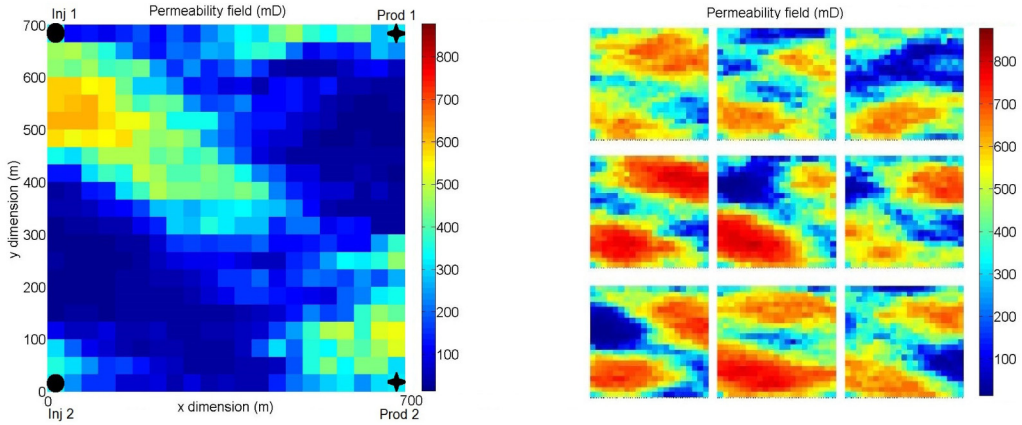

Figure 2—Left: Permeability (mD) and injectors/producers location for one realization. Right: Samples of the ensemble.

Generation of Reservoir Flow Patterns

This step involves the selection of production strategies and the simulation of reservoir flow patterns for the ensemble of realizations. The selection of the production strategy is not trivial issue, as it depends on the purpose of the flow characterization. The production strategy must be informative and rich enough to excite the dynamical variability of the ensemble. For the purpose of flow characterization for production optimization, we have several possibilities: The use of optimal production strategies for every model of the ensemble, the use of Nominal production, the use of Robust production, Reactive strategies and others.

Table 1—GEOLOGICAL AND FLUID PROPERTIES

Property	Value	Unit
k	13.74 - 876.61	mD
φ	0.17 - 0.37	-
ρ_w	1014	kg/m^3
ρ_o	859	kg/m^3
μ_w	1	cP
μ_o	5	cP
S_{wc}	0.2	-
S_{or}	0.2	-
k^0_{rw}	0.6	-
k^0_{ro}	0.9	-
n_w	4	-
n_o	4	-

Once the production strategy is defined, we can proceed with the simulation of reservoir flow patterns. The simulation involves the use of time stepping algorithms that generate discrete time trajectories for pressure and saturation. Nowadays, all the current reservoir simulators provide snapshot vectors for the states, for instance, the methodology requires a step where the vectorized trajectories from reservoir simulators X are translated to their corresponding tensor formulation S.

Flow Characterization Using Tensor Decompositions

In this work, data coming from the reservoir simulations are stored in large-scale spatial-temporal structures (*tensors*) while keeping the spatial nature of reservoir physics. Tensor decompositions offer a very flexible framework to handle multidimensional data structures and provide us with algorithms to find compact representations of these large-scale tensors. Tensor decomposition algorithms are applied to characterize reservoir simulations in the form presented in Eq. 7.

Evaluation of Dissimilarity Measures between Realizations

For a particular production strategy, the difference between the reservoir flow patterns of two geological realizations is an indicator of their dynamical variability. If we have the tensor formulation S of the reservoir flow patterns, it is possible to find reduced-rank approximations of $\hat{\mathbf{S}}$ and to use Eq. 11 to evaluate the dynamical dissimilarity between two different realizations.

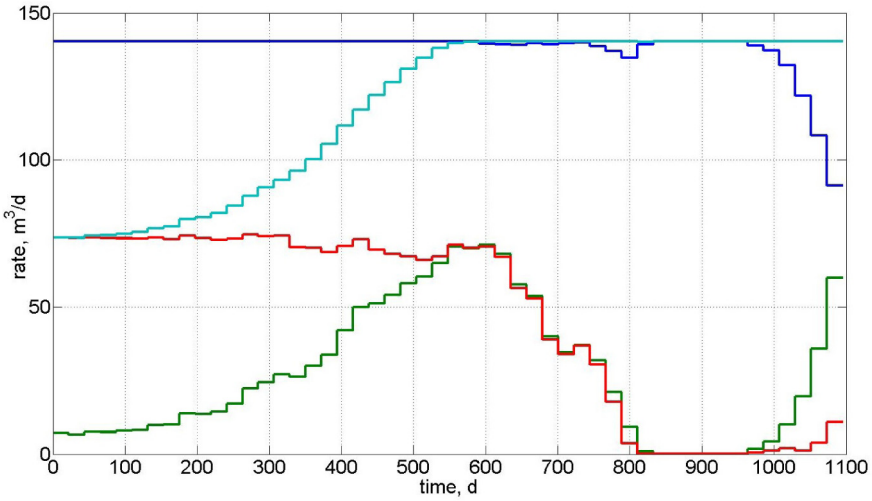

Figure 3—Production strategy. Blue: Injector rates 1. Green: Injector rates 2. Red: Producer rate 1. Cyan: Producer rate 2.

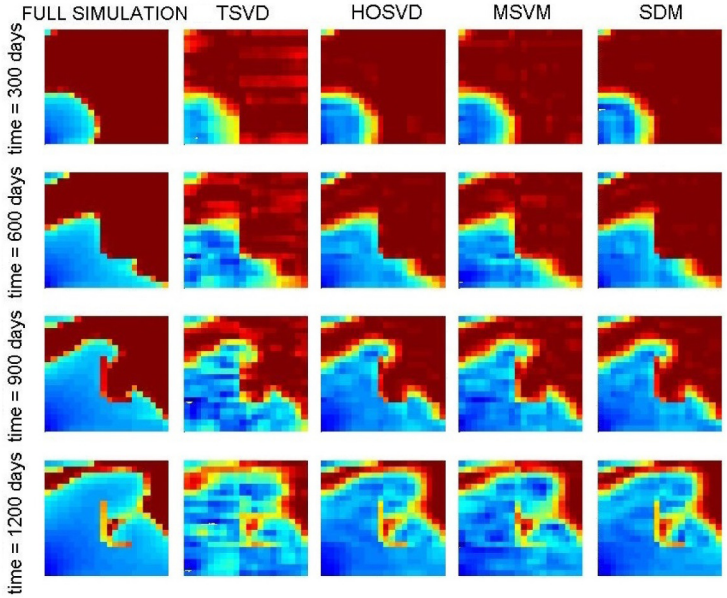

Figure 4—Time snapshots for oil saturation and (10, 10, 10) approximation computed using TSVD, HOSVD, MSVM and SDM.

Results

The Model

We study multi-phase fluid flow through heterogeneous porous media, with applications to oil reservoirs in a water flooding stage. We consider an ensemble of 2D oil reservoirs with a square geometry of length $L = 700$m, one layer of 2m thick, produced with 4 wells (2 *injectors*, 2 *producers).* The numerical model of one realization has 441 grid blocks of size 21m $\times$ 21m and the ensemble size $N_R = 1000$ realizations. A top view of some samples from ensemble, and well locations are shown in Fig. 2. The sequential solvers of MRST, see Lie et al. (2012), have been used to solve the pressure and saturation equations and the production has been simulated for a period of 1095 days, time step of 21.9 days. The adjoint module of MRST has been used to compute the optimal production strategies described in the next subsection. The physical parameters are presented in Table 1.

Table 2—RELATIVE APPROXIMATION ERROR FOR VARIOUS ALGORITHMS FOR TENSOR DECOMPOSITION

Tensor rank k_{rw}^0	TSVD	HOSVD	MSVM	SDM
(1, 1, 1)	0.2084	0.2085	0.2084	0.2084
(3, 3, 3)	0.1521	0.1370	0.1430	0.1364
(5, 5, 5)	0.1302	0.0911	0.1031	0.0928
(7, 7, 7)	0.1129	0.0718	0.0856	0.0732
(9, 9, 9)	0.0961	0.0562	0.0704	0.0579
(11, 11, 11)	0.0895	0.0428	0.0559	0.0443
(13, 13, 13)	0.0810	0.0345	0.0464	0.0355
(15, 15, 15)	0.0661	0.0279	0.0366	0.0289

Flow Characterization and Approximation: Single Reservoir Simulation

In this subsection, we characterize the saturation patterns of a single reservoir simulation by using tensor decomposition techniques. We build a 3D (2 *dimensions for the spatial domain*, 1 *dimension for the temporal domain*) tensor for the spatial-temporal evolution of oil saturation for one realization of the ensemble. We have used a gradient-based adjoint method to find an injection/production strategy with rate control that maximizes the NPV in Eq. 12, see Fig. 3. In this application case, the reservoir simulation contains 100 temporal snapshots. The data is stored in a tensor S of size $I = 21, J = 21, K = 100$. Time snapshots of the data and approximations are shown in Fig. 4 for different algorithms available in the literature.

We perform the truncation in Eq. 7 with $(\hat{I},\hat{J},\hat{K})$ where $\hat{I} = \hat{J} = \hat{K} = r$ and $1 \leq r \leq 10$. For different values of r, the relative approximation errors in Eq. 9 generated with different algorithms for tensor decompositions are presented in Table 2. We have found that some techniques are able to extract relevant information better than others. Both MSVM and SDM outperform the TSVD and their performance is comparable to the HOSVD. The slow rate of decrease of error in TSVD algorithm can be attributed to the restrictive space in which the algorithm searches it singular values, as it is a PARAFAC-type decomposition, see e.g., Kolda and Bader (2009). SDM, TSVD, MSVM perform better than HOSVD for the $r = 1$ approximation.

Flow Characterization and Approximation: Ensemble of Reservoir Simulations

Tensor decomposition algorithms can be adapted to support the computation of orthonormal basis functions for *n*-dimensional data arrays. In this subsection, we consider the ensemble of geological realizations, and we build a 4D (2 *dimensions for the spatial domain*, 1 *dimension for the temporal domain*, 1 *dimension for the models dimension*) tensor for the spatial-temporal evolution of oil saturation for every realization of the ensemble. We have used a gradient-based optimization, in which the gradients are computed with the adjoint method, to find injection/production strategies that maximize the NPV in Eq. 12 for every geological realization of the ensemble. In this

application case, every reservoir simulation contains 50 temporal snapshots. The data is stored in a 4D tensor S of size $I = 21, J = 21, K = 50, N_{ens} = 1000$. A schematic representation of such a data structure and its tensor decomposition is depicted in Fig. 5.

The HOSVD technique has been used to find the tensor representation in Eq. 4. As a consequence, a compact representation of the original tensor in terms of a reduced dimension of order 10 x 10 x 10 x 25 was found. Results from Figure 6 indicate that small sets of orthonormal basis functions are required to expand the spatial-temporal and model dimensions of the original 4D tensor, and to approximate it with an acceptable mismatch. The results so far suggest that tensor decompositions are a valuable tool for the characterization of saturation patterns, in terms of the reduced set of variables related to the orthonormal basis functions for every dimension. The HOSVD has proved to be computationally efficient to handle the large-scale data structure of the problem under consideration. Some of these orthonormal bases are presented in Fig. 6. We compute the truncation in Eq. 7 and the tensor S_e in Eq. 6 to visualize the level

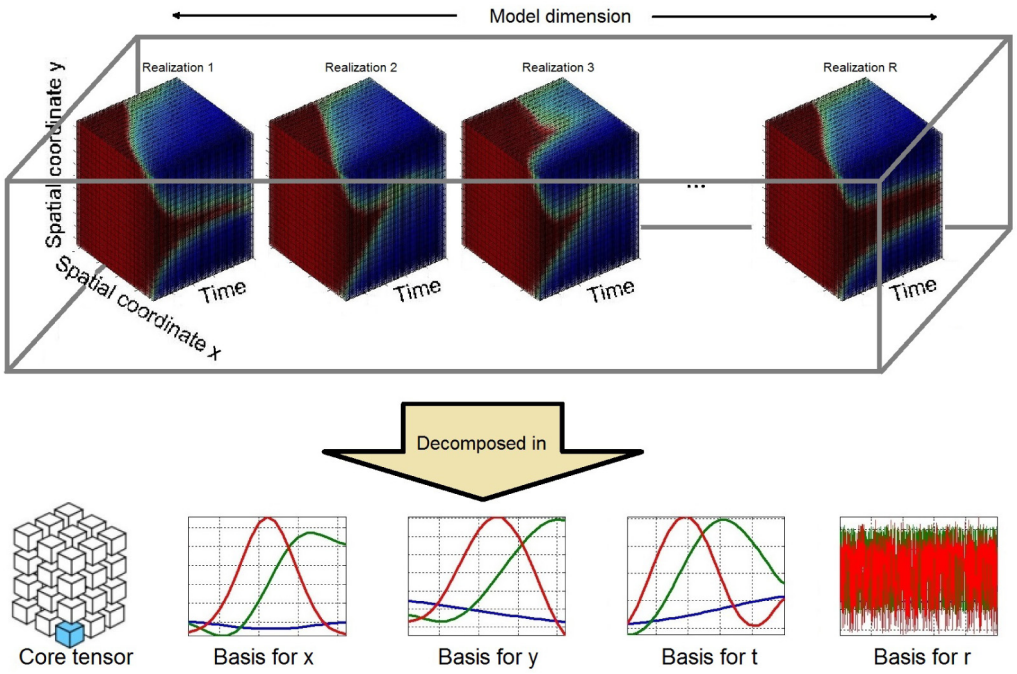

Figure 5—Schematic interpretation of a 4D tensor decomposition

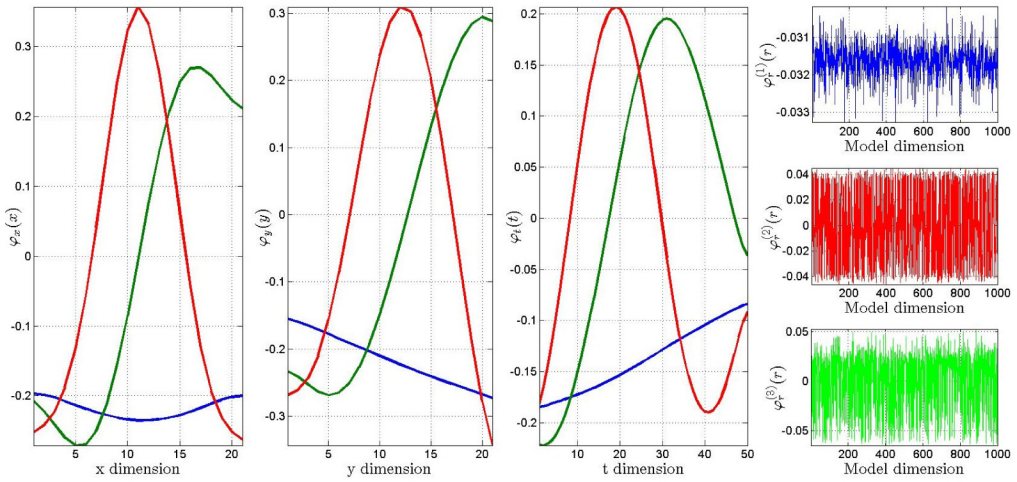

Figure 6—From left to right: Orthonormal basis functions for spatial x and y, temporal *t* and model spaces r. *Blue:* First basis. *Red:* Second basis. *Green:* Third basis.

of approximation achieved with this technique. Some temporal snapshots of S_e for different realizations are presented in Fig. 7.

Control-Relevant Ensembles for Production Optimization under Uncertainty

In the previous subsections, tensor decompositions have proved to be powerful techniques to extract the most relevant features from large-scale data arrays resulting from reservoir simulations, while preserving spatial and temporal structures. The truncated tensor in Eq. 7 is a lower-dimensional representation in terms of tensor rank, than the tensor in Eq. 6. Reservoir solutions usually demand huge computational resources (*processing times and storage*), thus, having compact representations of flow profiles enable the efficient computation the control-dissimilarity measure (saturation patterns) discussed in this paper.

In this subsection, we build a reduced size control-relevant ensemble, by characterizing the saturation patterns of every reservoir simulation of the ensemble with the aid of tensor decompositions. This

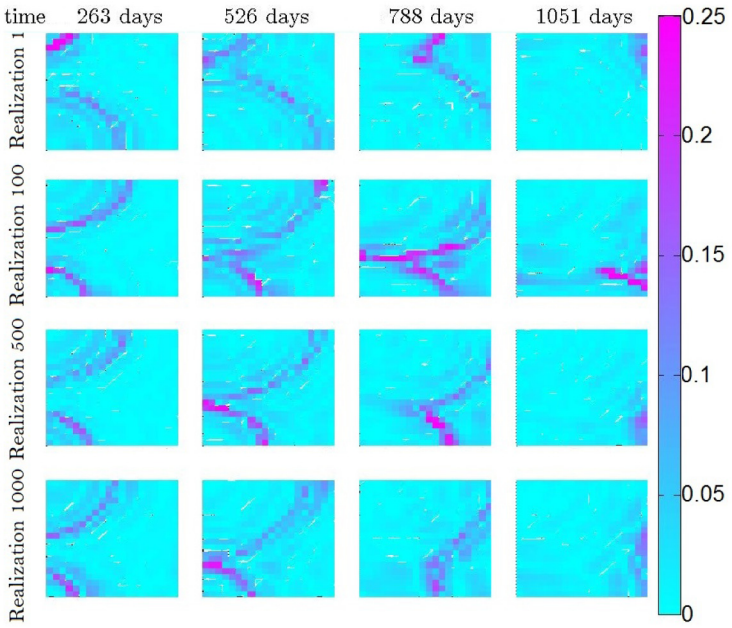

Figure 7—Time snapshots for S_ε with $r = 10$.

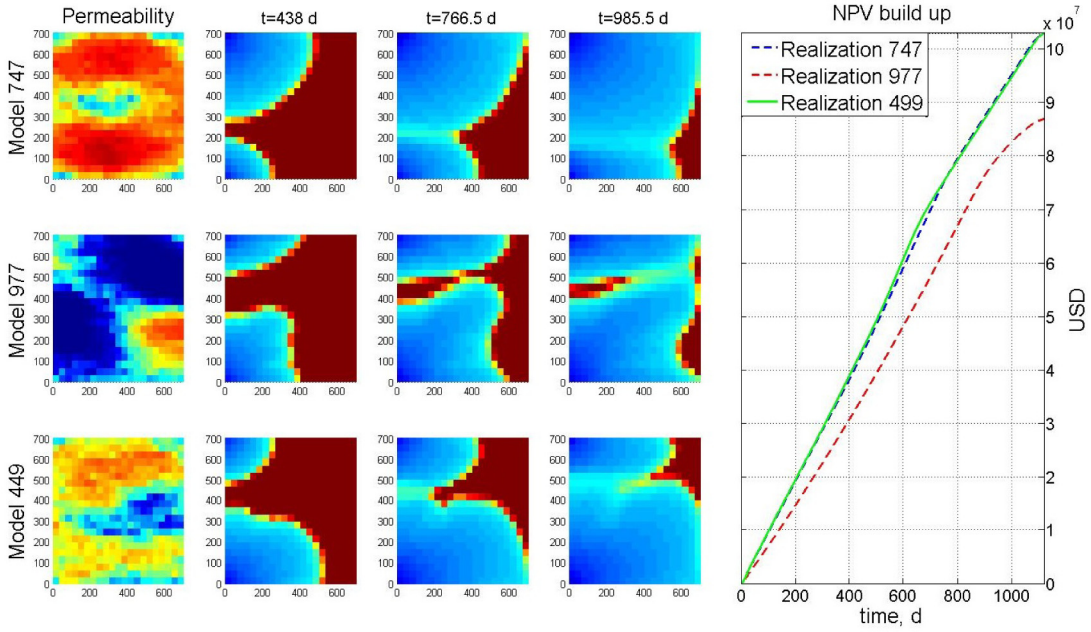

Figure 8—Saturation patterns and NPV build-up for realizations with highly dissimilar flow.

characterization generates compact representations of reservoir flow profiles which are used to measure the dynamical dissimilarity between reservoir models. With this approach we select, in the low-order space, realizations from a large ensemble that are dynamically/flow relevant in an optimized setting. In a dynamical environment (*flow simulations*), realizations have less variability than in a static setting (*geological realizations).* Hence, we construct a reduced size ensemble of geological realizations that possesses similar performance than the original ensemble for purpose of production optimization.

RO can be used to design production strategies for water flooding, when uncertainty is represented by an ensemble of geological realizations. In practice, models and ensembles might be large-scale, and RO techniques may not be computationally feasible or require a large amount of computational resources and

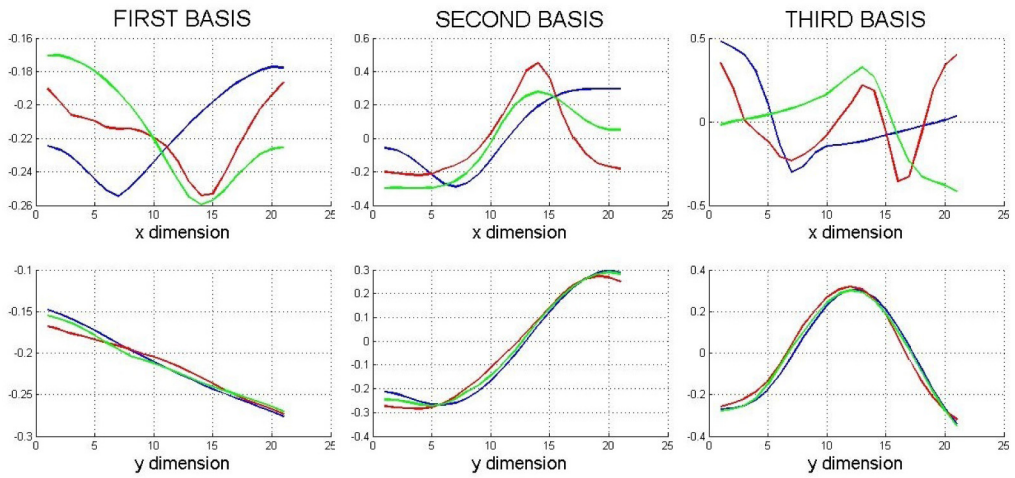

Figure 9—Orthonormal basis functions for the spatial spaces for three realizations with different saturation patterns. Blue: Realization 747. Red: Realization 977. Green: Realization 449.

time in order to obtain a production strategy. Yeh et al. (2014) have provided evidence that only a few flow-relevant realizations are needed for model maturation under uncertainty. In this subsection, we demonstrate that the use of flow-relevant ensembles may increase the computational feasibility of techniques for production optimization under uncertainty.

Data generation We have considered the ensemble of realizations with size $N_R = 1000$ presented before and in Fig. 2. We use the data from the previous subsection, where the flow profiles of each of the realizations are simulated with their own optimal (*maximum NPV*) production strategies.

Flow characterization and approximation: Ensemble of realizations. We use our in-house built SDM algorithm to decompose and characterize the 3D tensor formulation of the reservoir flow patterns for every reservoir model of the ensemble. We perform modal truncation of the different dimensions with $r = 10$.

Data comparison, visualization and model selection. Once reservoir flow patterns are represented in their tensor formulation, models are compared in terms of their dissimilarity of saturation patterns in the low dimensional space using the dissimilarity measure in Eq. 11. In Fig. 8 we present the temporal evolution of saturation and NPV of three realizations of the ensemble with high dissimilarity in their saturation patterns. Their corresponding orthonormal basis functions are presented in Fig. 9.

In Fig. 10 we present the temporal evolution of saturation and NPV of three realizations of the ensemble with low dissimilarity in their saturation patterns. Their corresponding orthonormal basis functions are presented in Fig. 11.

On one hand, in Fig. 9, some orthonormal basis functions of the control-relevant reservoir flow patterns for three realizations with different saturation patterns are presented. It is clear that the more different the saturation patterns are, the more dissimilar the orthonormal basis functions for each dimension are. This evidence indicates that dissimilarities in the reduced-order spaces are correlated to dissimilarities in the saturation patterns. On the other hand, for models with similar flow-relevant reservoir flow patterns as the ones presented in Fig. 10, the orthonormal basis functions are quite similar, and a whole set of similar saturation patterns can be characterized with the same reduced set of orthonormal basis functions. The realizations used for illustration of similar and dissimilar reservoir flow patterns in Figs. 10 and 8 are also shown in the MDS plot in Fig. 12.

To visualize dissimilarity between the control-relevant saturation patterns from the whole ensemble of realizations in the low dimensional space, we use the MDS technique. Numerical techniques such as MDS define a metric space where distance between points in the map represent dissimilarities in terms of

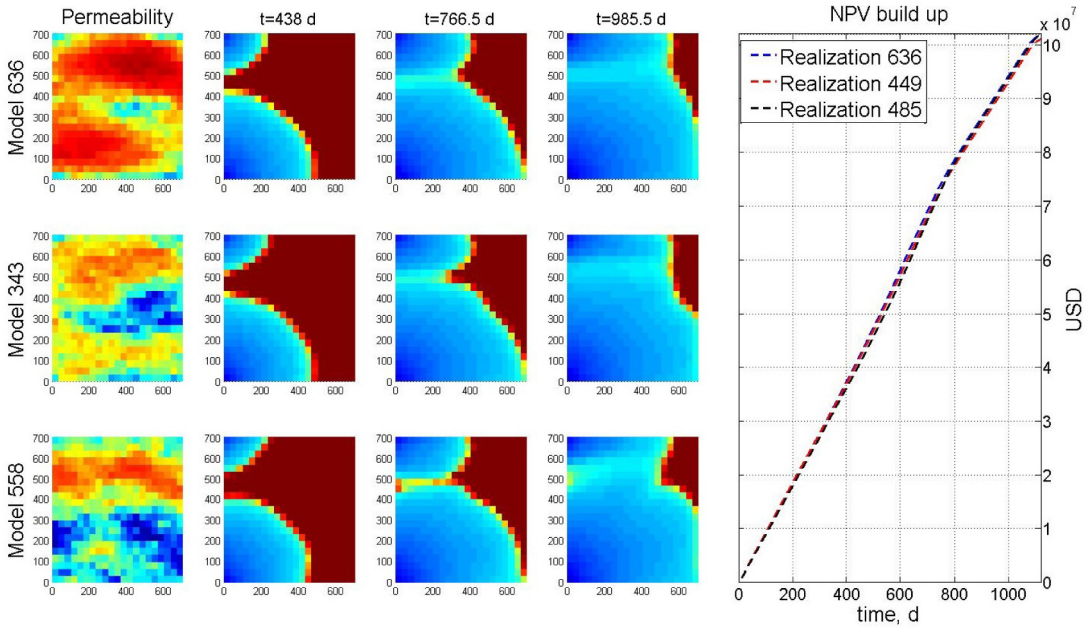

Figure 10—Saturation patterns and NPV build-up for realizations with similar flow.

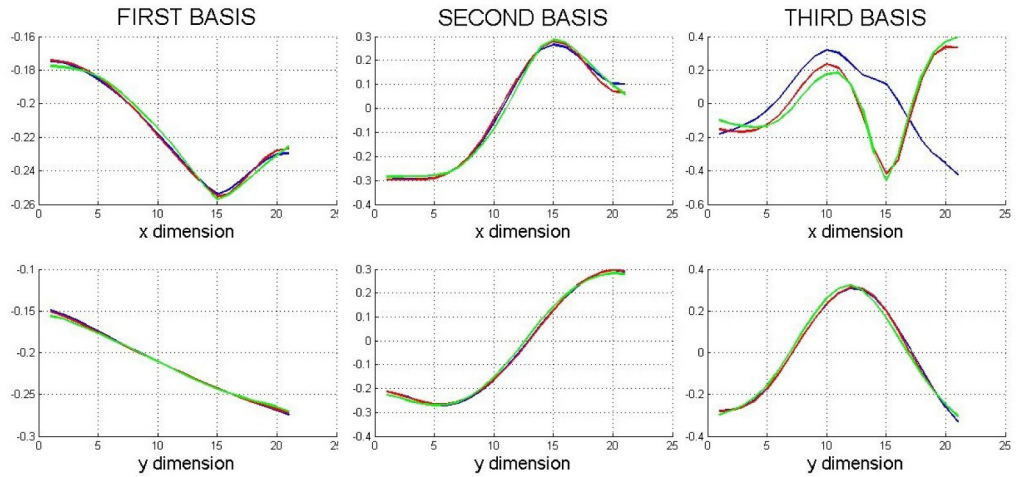

Figure 11—Orthonormal basis functions for the spatial spaces for realizations with similar saturation patterns. Blue: Realization 636. Red: Realization 343. Green: Realization 558.

saturation patterns for the different geological realizations. Although realizations from the ensemble might look different from a geological perspective, their variation in terms of dynamical behavior, i.e. saturation patterns, can be smaller. Therefore, clusters of models with similar saturation patterns usually appear in the metric space map. The MDS map for the dissimilarity matrix in Eq. 11 is presented in Fig. 12.

Representative models are sampled from the metric space map in order to reduce the ensemble size and to select the realizations that are significantly dynamically dissimilar. We can screen models by either selecting realizations that are close to measurements, selecting clusters centroids or by generating representative realizations using post-image techniques. We have selected 50 realizations close to the centroids of the clusters in the MDS map to construct the control-relevant ensemble.

Production optimization with control-relevant ensemble. A production strategy that maximizes the average value of NPV using the control-relevant ensemble is generated with RO techniques. We use a gradient-based methodology to compute the solutions, (see Jansen (2011) for a review) with the objective

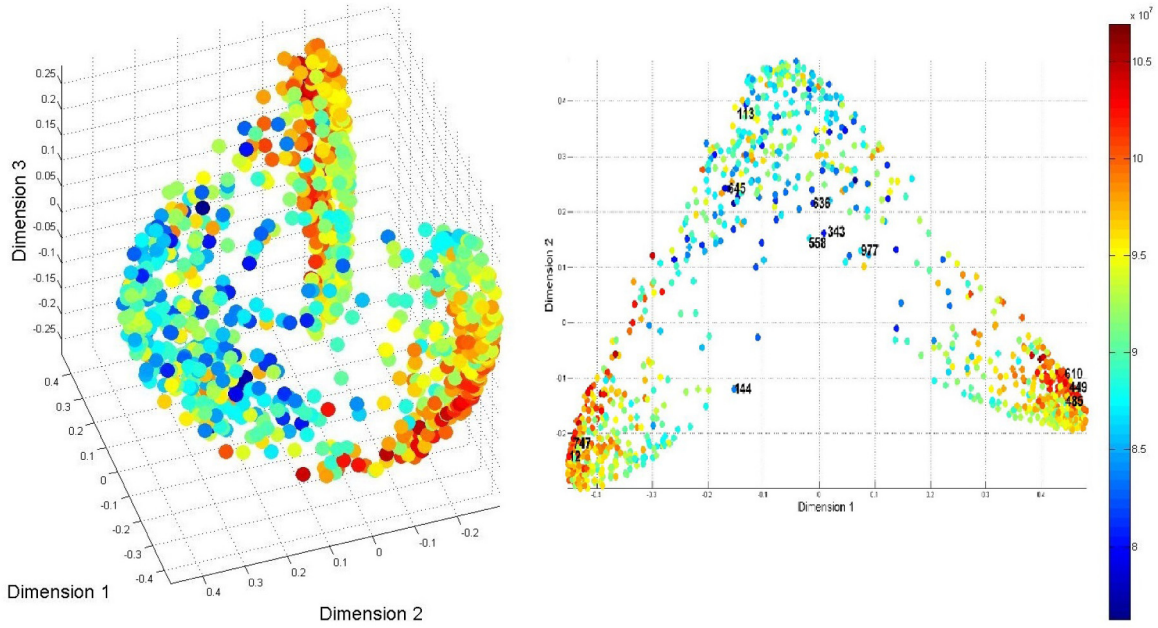

Figure 12—MDS for the low dimensional flow profiles from the ensemble. ***Colors represent final NPV.*** **Left: 3D map. Right: 2D map**

function and gradients described in Eq. 12 and 13, and robust strategies are generated for the original (N_r = 1000) and the flow-relevant ensemble (N_r = 50). The production strategies are presented in Fig. 13.

We simulate the full ensemble with the production strategies in Fig. 13. A distribution of the final NPV for the full ensemble with the two different strategies is presented in Fig. 14. After the clustering of realizations with similar control-relevant reservoir flow patterns, the production strategy for the reduced ensemble in Fig. 13 resembles the production strategy generated using the full ensemble of realizations, and therefore both production strategies have a similar NPV distribution when applied to the full ensemble of realizations.

Discussion

In the previous section, a flow-based dissimilarity measure has been used for generating a control-relevant ensemble for RO, where the reservoir models are clustered according to their similarity with respect to their reservoir flow patterns. We have computed the dissimilarity between 3D reservoir flow patterns by using Eq. 11, however, the tensor formulation can be exploited for efficient computation of flow-based dissimilarity measures. As an alternative method for evaluating dissimilarity between models, a 4D structure composed by an ensemble of reservoir simulations can be decomposed as it is depicted in Fig. 5. If the most relevant basis function for the model (Nr = 50) dimension is used only to span the model space, we are able to reconstruct approximate 3D structures for the individual reservoir flow patterns of the ensemble. Hence, we are able to efficiently evaluate flow-based dissimilarity measures between realization based on the elements σ_{ijkl} of the 4D core tensor.

The application case discussed in the previous section implies the computation of the optimal production strategy for every reservoir model of the ensemble. However, we may also consider the use of an unique production strategy to generate an ensemble of reservoir flow patterns, and select the geological realizations that prove to substantially contribute to the dynamical variability using the tensor-based methods described in the previous sections.

The Effect of the Production Strategy on the Generation of Flow-Relevant Ensembles

In order to study and quantify the effects of different production strategies on the dynamical variability of the ensemble, we have generated reservoir flow patterns for the ensemble by using an unique control

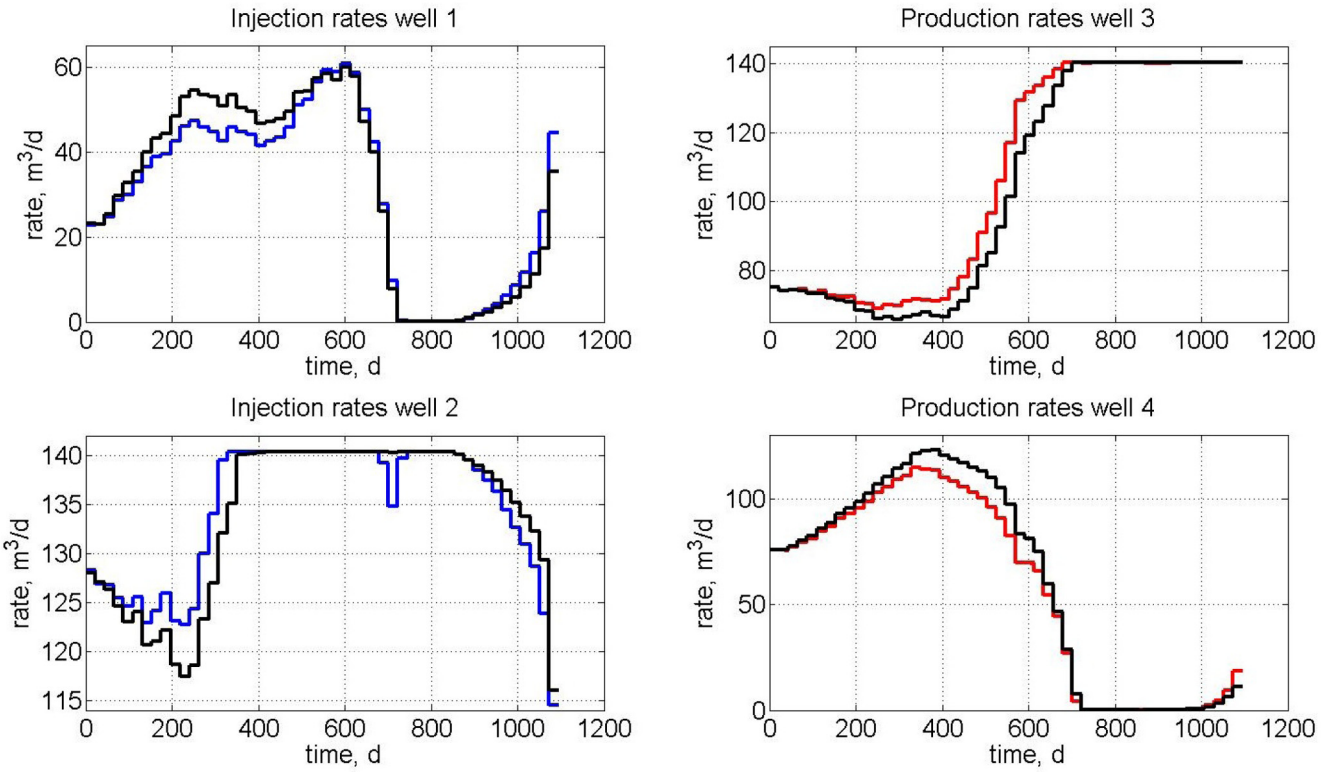

Figure 13—Injection and production rates for RO. *Blue/Red:* Full ensemble (N_R = 1000). *Black:* Strategy with control-relevant ensemble (N_R = 50)

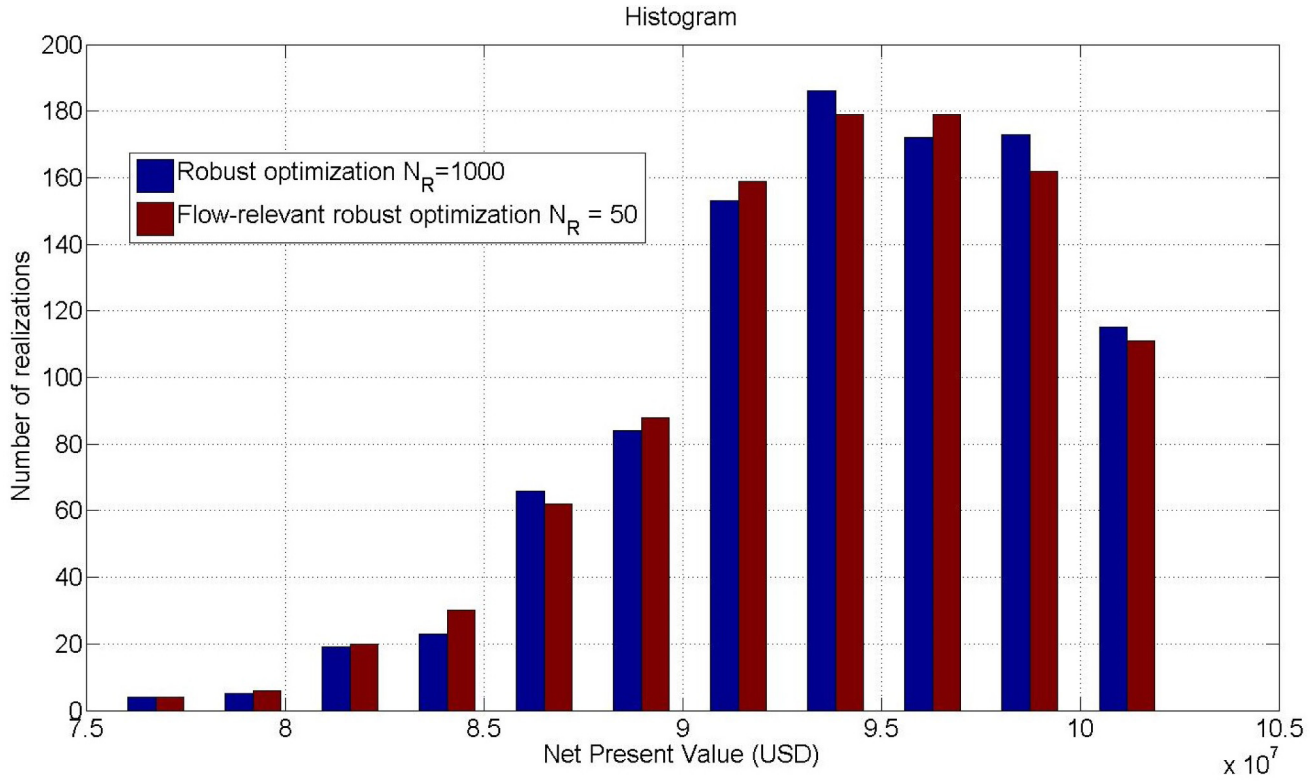

Figure 14—Distribution of NPV over the ensembles.

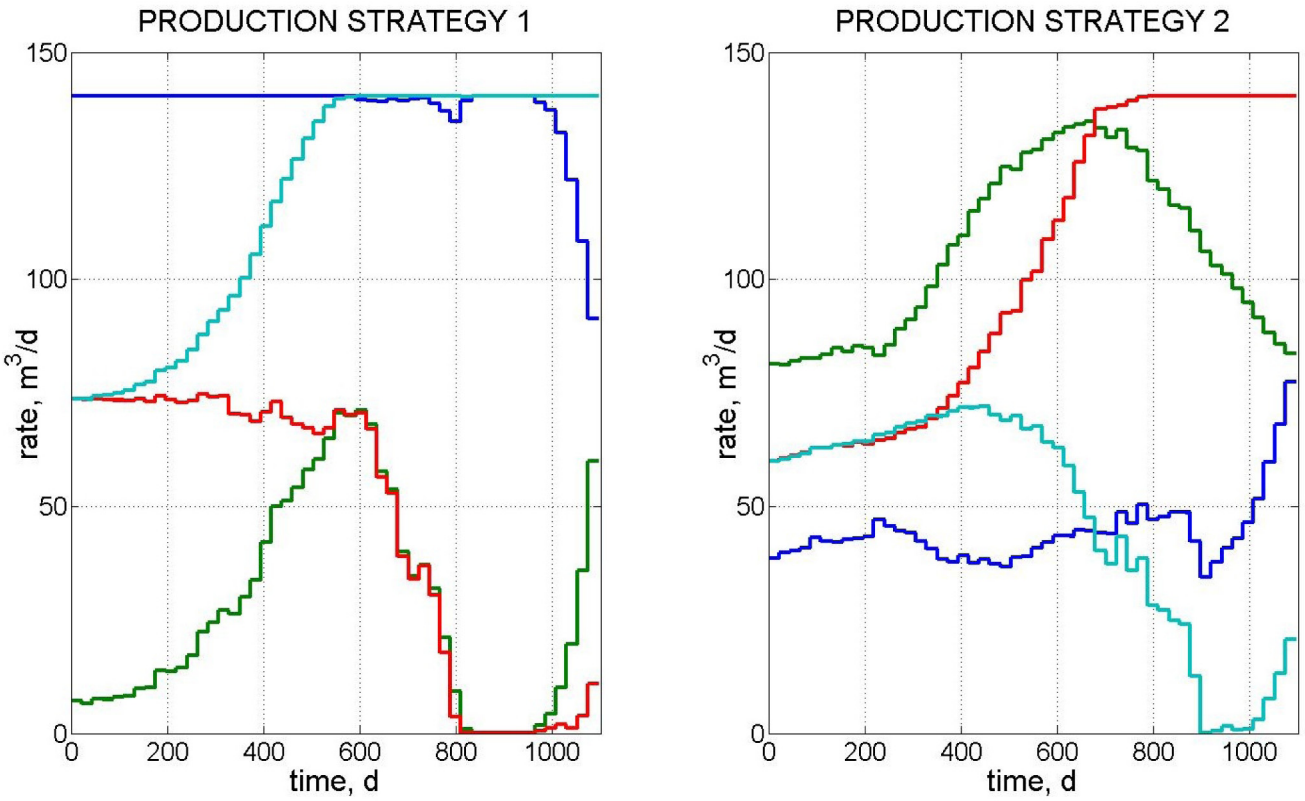

Figure 15—Left: Optimal production strategy for Reservoir model 1. Right: Optimal production strategy for Reservoir model 2. Blue: Injector rates 1. Green: Injector rates 2. Red: Producer rate 1. Cyan: Producer rate 2.

input. We have performed Nominal Optimization over the ensemble with the two production strategies depicted in Fig. 15, which correspond to the optimal production strategies for the reservoir realizations 1 and 2.

We have used the methodology described in the previous section to characterize the ensemble of reservoir flow patterns in the low-dimensional space. This allows the construction of the MDS maps to visualize the dynamical variability of the ensemble.

In Fig. 16, the MDS maps of the flow-relevant dissimilarity for the Nominal Optimization experiments are presented. We have indicated with a number the ensemble members that have been subject of study in the previous section. The shapes of the MDS maps for both Nominal Optimizations and the MDS map in Fig. 12 present significant differences, however, we have found evidence of similar clustering patterns with respect to the dynamical behavior and financial performance in both experiments. To exemplify this observation, the models with similar dynamical behavior in Fig. 10, are again clustered in the MDS maps for the Nominal Optimization experiments in Fig. 16, indicating that the dynamical variability of the ensemble remains almost invariant for different choices of production strategies. For the MDS plots in Fig. 16, there is evidence of the connection between the reservoir flow patterns generated with the Nominal strategy and the NPV, as clusters of models with similar dynamical performance have also similar financial performance. This fact is a direct consequence of the uniqueness of the production strategy used for the simulation.

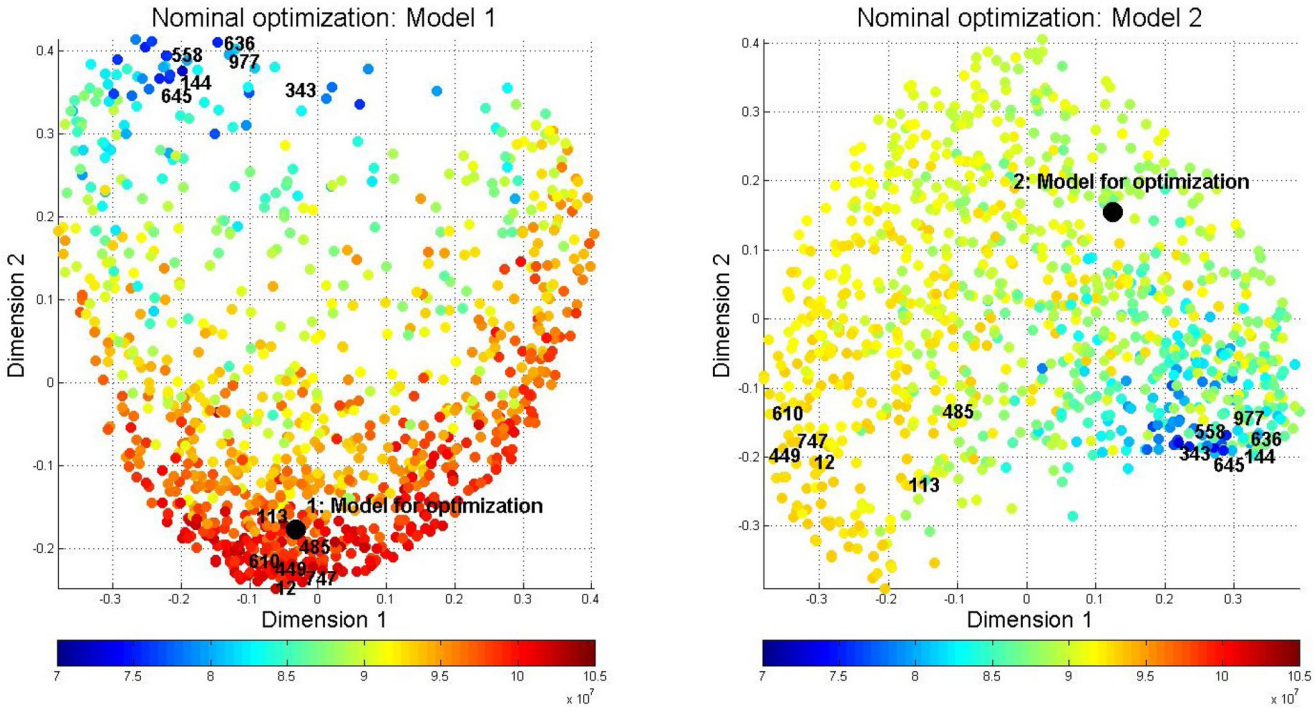

Figure 16—MDS for Nominal Optimization. Left: Optimal production strategy for Reservoir model 1 applied to the ensemble. Right: Optimal production strategy for Reservoir model 2 applied to the ensemble. ***Color scale represent final NPV.***

Conclusion

We have investigated the potential use of spatial-temporal tensor decompositions for the characterization and approximation of saturation patterns, which has been used for the efficient computation of flow-relevant dissimilarity measures between reservoir models.

Tensor decompositions are efficient techniques for the characterization of reservoir flow patterns in terms of a reduced set of orthonormal basis functions. They allow the reduction of large-scale spatial-temporal data structures obtained from reservoir simulations with an efficiency close to 98%. The low-dimensional representations of flow profiles obtained with tensor decompositions have been successfully applied in the evaluation of control-relevant dissimilarity between models.

For the purpose of model-based recovery optimization under uncertainty, only a few flow-relevant realizations with distinctive flow properties are needed to efficiently perform robust optimization. For the application case in this paper, the dynamic variability, represented by the reduced-order ensemble, was much smaller than the static variability, represented by the original ensemble of geological realizations.

The methods used in this paper can be extended to problems where characterization of spatial-temporal evolution of saturations is required to reduce the computational loads of the production optimization procedures, and for model order reduction.

Acknowledgements

The authors acknowledge financial support from the Recovery Factory program sponsored by Shell Global Solutions International.

Nomenclature

k= permeability

k_{rw}^0 = water en point relative permeability

k_{ro}^0 =

oil en point relative permeability
μ_w = water viscosity
μ_o = oil viscosity
n_w = Corey exponent water
n_o = Corey exponent oil
φ = porosity
ρ_w = water density
ρ_o = oil density
S_{wc} = connate water saturation
S_{or} = residual oil saturation

References

Afra, S., Gildin, E. 2013. Permeability parametrization using Higher Order Singular Value Decomposition (HOSVD). In: 12th International Conference on Machine Learning and Applications (ICMLA). **2**: 188–193. DOI: 10.1109/icmla.2013.121.

Afra, S., Gildin, E., Tarrahi, M. 2014. Heterogeneous reservoir characterization ussing efficient parameterization through Higher Order SVD (HOSVD). In: American Control Conference. Portland, 4–6 September. DOI: 10.1109/acc.2014.6859246.

Alpak, F.O., Barton, M.D., Caers, J. 2010. A flow-based pattern recognition algorithm for rapid quantification of geologic uncertainty. *Computational Geosciences* **14** (4): 603–621. DOI: 10.1007/s10596–009–9175–5.

Aziz, K., Settari, A. 1979. *Petroleum reservoir simulation*. Vol. **476**. London, Applied Science Publishers

Borg, I., Groenen, P.J.F. 2005. *Modern multidimensional scaling: Theory and applications*. Springer. DOI: 10.4324/9780203767719.

Caers, J., Park, K., Scheidt, C. 2010. Modeling uncertainty of complex earth systems in metric space. In: *Handbook of Geomathematics*. Springer. 865–889. DOI: 10.1007/978–3–642–01546–5–29.

Cardoso, M.A., Durlofsky, L.J., Sarma, P. 2009. Development and application of reduced-order modeling procedures for subsurface flow simulation. *International Journal for Numerical Methods in Engineering* **77** (9): 1322–1350. DOI: 10.1002/nme.2453.

Chen, C., Li, G., Reynolds, A., et alet al. 2012. Robust constrained optimization of short-and long-term net present value for closed-loop reservoir management. *SPEJ* **17** (03): 849–864. DOI: 10.2118/141314–PA.

Chen, Y., Oliver, D.S., Zhang, D., et alet al. 2009. Efficient ensemble-based closed-loop production optimization. *SPEJ* **14** (04): 634–645. DOI: 10.2118/112873–pa.

De Lathauwer, L., De Moor, B., Vandewalle, J. 2000a. A multilinear singular value decomposition. *SIAM Journal on Matrix Analysis and Applications* **21** (4): 1253–1278. DOI: 10.1137/s0895479896305696.

De Lathauwer, L., De Moor, B., Vandewalle, J. 2000b. On the best rank-1 and rank-(r_1, r_2,. . ., r_n) approximation of higher-order tensors. *SIAM Journal on Matrix Analysis and Applications* **21** (4): 1324–1342. DOI: 10.1137/s0895479898346995.

Durlofsky, L.J. 2005. Upscaling and gridding of fine scale geological models for flow simulation. In: 8th International Forum on Reservoir Simulation. Iles Borromees, Stresa, Italy, 20–24 June.

Eckart, C., Young, G. 1936. The approximation of one matrix by another of lower rank. *Psychometrika* **1** (3): 211–218. DOI: 10.1007/bf02288367.

Fonseca, R.M., Leeuwenburgh, O., Della Rossa, E., Van den Hof, P.M.J., Jansen, J.D. 2015.

Ensemble-based multi-objective optimization of on-off control devices under geological uncertainty, Paper 173268-MS presented at the 2015 SPE Reservoir Simulation Symposium, 22-25 February, Houston, USA.

Gildin, E., Afra, S. 2014. Efficient inference of reservoir parameter distribution utilizing higher order svd reparameterization. In: ECMOR XIV-14th European conference on the mathematics of oil recovery. Catania, Italy, 8–11 September. DOI: 10.3997/2214-4609.20141826.

Heijn, T., Markovinovic, R., Jansen, J.D., et alet al. 2004. Generation of low-order reservoir models using system-theoretical concepts. *SPEJ* **9** (2): 202–218. DOI: 10.2118/88361–pa.

Insuasty, E., Van den Hof, P.M.J., Weiland, S., Jansen, J.D. 2015. Tensor-based reduced order modeling in reservoir engineering: An application to production optimization. Paper submittetd to the 2nd IFAC Workshop on Automatic Control in Offshore Oil and Gas Production. Florianopolis, Brazil, 27–29 May.

Jansen, J.D. 2011. Adjoint-based optimization of multi-phase flow through porous media–a review. *Computers & Fluids* **46** (1): 40–51. DOI: 10.1016/j.compfluid.2010.09.039.

Jansen, J.D., Bosgra, O.H., Van den Hof, P.M.J. 2008. Model-based control of multiphase flow in subsurface oil reservoirs. *Journal of Process Control* **18** (9): 846–855. DOI: 10.1016/j.jprocont.2008.06.011.

Jansen, J.D., Douma, S.D., Brouwer, D.R., Van den Hof, P.M.J., Bosgra, O.H., Heemink, A.W. 2009. Closed-loop reservoir management. In: SPE Reservoir Simulation Symposium. Society of Petroleum Engineers, The Woodlands, Texas, 2–4 February. DOI: 10.2118/119098-ms.

Kaleta, M.P., Hanea, R.G., Heemink, A.W., Jansen, J.D. 2011. Model-reduced gradient-based history matching. *Computational Geosciences* **15** (1): 135–153. DOI: 10.1007/s10596–010–9203–5.

Kolda, T.G., Bader, B.W. 2009. Tensor decompositions and applications. *SIAM Review* **51** (3): 455–500. DOI: 10.1137/07070111x.

Krogstad, S. 2011. A sparse basis pod for model reduction of multiphase compressible flow. In: SPE Reservoir Simulation Symposium. The Woodlands, Texas, 21–23 February. DOI: 10.2118/141973-ms.

Lie, K.-A., Krogstad, S., Ligaarden, I.S., Natvig, J.R., Nilsen, H.M., Skaflestad, B. 2012. Open-source matlab implementation of consistent discretisations on complex grids. *Computational Geosciences* **16** (2): 297–322. DOI: 10.1007/s10596–011–9244–4.

Markovinovic, R., Jansen, J.D. 2006. Accelerating iterative solution methods using reduced-order models as solution predictors. *International Journal for Numerical Methods in Engineering* **68** (5): 525–541. DOI: 10.1002/nme.1721.

Sarma, P., Durlofsky, L.J., Aziz, K. 2008. Computational techniques for closed–loop reservoir modeling with application to a realistic reservoir. *Petroleum Science and Technology* **26** (10-11): 1120–1140. DOI: 10.1080/10916460701829580.

Shekhawat, H.S., Weiland, S. 2014. On the problem of low rank approximation of tensors. In: 21st International Symposium on Mathematical Theory of Networks and Systems. Groningen, The Netherlands, 7–11 July.

Suzuki, S., Caumon, G., Caers, J. 2008. Dynamic data integration for structural modeling: model screening approach using a distancebased model parameterization. *Computational Geosciences* **12** (1): 105–119. DOI: 10.1007/s10596–007–9063–9.

Tavakoli, R., Reynolds, A.C., et alet al. 2010. History matching with parametrization based on the SVD of a dimensionless sensitivity matrix. *SPEJ* **15** (02): 495–508. DOI: 10.2118/118952–pa.

Vakili-Ghahani, S.A., Jansen, J.D. 2012. A system-theoretical approach to selective grid coarsening of reservoir models. *Computational Geosciences* **16** (1): 159–176. DOI: 10.1007/s10596–011–9260–4.

Van Doren, J.F.M., Van den Hof, P.M.J., Bosgra, O.H., Jansen, J.D. 2013. Controllability and observability in two-phase porous media flow. *Computational Geosciences* **17** (5): 773–788. DOI: 10.1007/s10596−013–9355–1.

Van Doren, J.F.M., Van den Hof, P.M.J., Jansen, J.D., Bosgra, O.H. 2011. Parameter identification in large-scale models for oil and gas production. In: The 18th IFAC World Congress. Milano, Italy. 28 August - 2 September. DOI: 10.3182/20110828−6–it–1002.01823.

Van Essen, G.M., Zandvliet, M.J., Van den Hof, P.M.J., Bosgra, O.H., Jansen, J.D. 2009. Robust waterflooding optimization of multiple geological scenarios. *SPEJ* **14** (01): 202–210. DOI: 10.2118/102913–ms.

Weiland, S., Van Belzen, F. 2010. Singular value decompositions and low rank approximation of tensors. *IEEE Transactions on Signal Processing* **58** (3): 1171–1182. DOI: 10.1109/tsp.2009.2034308.

Yasari, E., Pishvaie, M.R., Khorasheh, F., Salahshoor, K., Kharrat, R. 2013. Application of multi-criterion robust optimization in waterflooding of oil reservoir. *Journal of Petroleum Science and Engineering* **109**: 1–11. DOI: 10.1016/j.petrol.2013.07.008.

Yeh, T.-H., Jimenez, E., Van Essen, G., Chen, C., Jin, L., Girardi, A., Gelderblom, P., Horesh, L., Conn, A.R., et alet al. 2014. Reservoir uncertainty quantification using probabilistic history matching workflow. In: SPE Annual Technical Conference and Exhibition. Amsterdam, The Netherlands, 27–29 October. DOI: 10.2118/170893-ms.